Modern radio engineering and telecommunication systems

Современные радиотехнические и телекоммуникационные системы

UDC 621.396.969
https://doi.org/10.32362/2500-316X-2024-12-4-70-83
EDN QDYIBS

RESEARCH ARTICLE

Principles of construction of nanosatellite radar systems based on global navigation satellite system reflectometry

Alexander V. Ksendzuk [1, @], Vyacheslav F. Fateev [2]

[1] *MIREA – Russian Technological University, Moscow, 119454 Russia*
[2] *Scientific and Technical Center of Metrology in Gravimetry, VNIIFTRI, Solnechnogorsk, Moscow oblast, 141570 Russia*
[@] *Corresponding author, e-mail: ks_alex@mail.ru*

Abstract

Objectives. The development of radar remote sensing systems based on the reception of signals of navigation satellite systems reflected from the surface enables a constellation of nanosatellites to be deployed, in order to perform radar surveying of the Earth's surface. The aim of this work is to develop the principles of construction of onboard bistatic remote sensing systems on nanosatellites, in order to assess the energy potential and possibilities for its increase.

Methods. The optimal processing method in onboard bistatic radar systems is a development of known analytical methods of optimal processing in monostatic systems. The calculation of the energy potential is based on the experimental data obtained by other authors.

Results. The utilization of signals from navigation satellite systems for surface sensing is a promising and developing area. The USA and China have deployed satellite constellations to perform remote sensing using reflected signals of navigation satellites. An algorithm for optimal processing in such systems, which realizes the principle of aperture synthesis, was developed, and the energy potential of bistatic synthetic aperture radar was calculated. In order to achieve this processing, the proposed scheme uses a standard navigation receiver to form reference signals.

Conclusions. The application of optimal processing methods in bistatic radar enables a synthetic aperture based on scattered satellite navigation system signals. In order to improve the accuracy of estimates, the signal-to-noise ratio needs to be increased by combining coherent accumulation (aperture synthesis) and incoherent accumulation (aggregating measurements from different spacecraft). The signal processing methods and receiver structure proposed in this work onboard nanosatellites allow aperture synthesis to be achieved with realizable hardware requirements.

Keywords: bistatic radar, synthetic aperture, navigation satellite, optimal processing

• **Submitted:** 29.11.2023 • **Revised:** 02.02.2024 • **Accepted:** 24.05.2024

For citation: Ksendzuk A.V., Fateev V.F. Principles of construction of nanosatellite radar systems based on global navigation satellite system reflectometry. *Russ. Technol. J*. 2024;12(4):70–83. https://doi.org/10.32362/2500-316X-2024-12-4-70-83

Financial disclosure: The authors have no a financial or property interest in any material or method mentioned.

The authors declare no conflicts of interest.

НАУЧНАЯ СТАТЬЯ

Принципы построения бортовых радиолокационных систем наноспутников, основанных на приеме отраженных сигналов спутниковых навигационных систем

А.В. Ксендзук [1, @],
В.Ф. Фатеев [2]

[1] *МИРЭА – Российский технологический университет, Москва, 119454 Россия*
[2] *Всероссийский научно-исследовательский институт физико-технических и радиотехнических измерений, Солнечногорск, Московская область, 141570 Россия*
[@] *Автор для переписки, e-mail: ks_alex@mail.ru*

Резюме

Цели. Создание радиолокационных систем дистанционного зондирования, основанных на приеме отраженных от поверхности Земли сигналов навигационных спутниковых систем, позволяет развернуть группировку наноспутников радиолокационного обзора земной поверхности. Целью работы является развитие принципов построения бортовых бистатических систем дистанционного зондирования на сверхмалых космических аппаратах, оценка энергетического потенциала и возможностей его увеличения.

Методы. Оптимальный метод обработки в бортовых бистатических радиолокационных системах (ББРЛС) является развитием известных аналитических методов оптимальной обработки в моностатических системах. Расчет энергетического потенциала основывается на исходных данных, полученных в ходе экспериментальных исследований других авторов.

Результаты. Использование сигналов навигационных спутниковых систем для зондирования поверхности является перспективным, развивающимся направлением. США и Китаем развернуты спутниковые группировки, осуществляющие дистанционное зондирование по отраженным сигналам навигационных спутников. Разработан алгоритм оптимальной обработки в таких системах, реализующий принцип синтезирования апертуры, рассчитан энергетический потенциал бистатической радиолокационной системы с синтезированием апертуры антенны. Для реализации обработки предложена схема с использованием стандартного навигационного приемника, который используется для формирования опорных сигналов.

Выводы. Применение методов оптимальной обработки в ББРЛС позволяет синтезировать радиолокационное изображение по сигналам космических навигационных аппаратов. Для повышения точности оценок необходимо увеличить отношение сигнал/шум за счет сочетания когерентного накопления (синтез апертуры) и некогерентного накопления (комплексирование измерений по разным космическим аппаратам). Предложенные в работе методы обработки сигналов и структура приемника на борту сверхмалого космического аппарата позволяют реализовать синтезирование апертуры при реализуемых требованиях к аппаратной части.

Ключевые слова: бистатическая радиолокационная система, синтез апертуры, навигационный спутник, оптимальная обработка

• **Поступила:** 29.11.2023 • **Доработана:** 02.02.2024 • **Принята к опубликованию:** 24.05.2024

Для цитирования: Ксендзук А.В., Фатеев В.Ф. Принципы построения бортовых радиолокационных систем наноспутников, основанных на приеме отраженных сигналов спутниковых навигационных систем. *Russ. Technol. J*. 2024;12(4):70–83. https://doi.org/10.32362/2500-316X-2024-12-4-70-83

Прозрачность финансовой деятельности: Авторы не имеют финансовой заинтересованности в представленных материалах или методах.

Авторы заявляют об отсутствии конфликта интересов.

INTRODUCTION

Space-based Earth remote sensing (ERS) radiolocation systems (radars) make it possible to monitor the Earth's surface and objects located on it regardless of weather conditions and time of day.

The possibility of recording large areas, incl. in hard-to-reach areas, high efficiency, operation at any time of the day and in any weather, have led to the deployment of satellite constellations (more than 80 spacecrafts (SC) at the end of 2023). Their objective is to resolve the following tasks: constructing radar images of the surface, detecting stationary and moving objects, construction of surface relief maps, assessment of the state of the water surface (currents, near-shore wind, wave intensity), monitoring of hurricanes and tsunamis, monitoring and forecasting of ice conditions, incl. in the Arctic zone, etc. [1].

Currently, most spaceborne remote sensing radars are monostatic radars with radar antenna aperture synthesis (synthetic-aperture radar (SAR)). The bistatic configuration has been achieved only in the form of TanDem-X (EADS Astrium, Germany) [1].

In active SAR, the possibilities of reducing the size, mass, and power consumption are limited by the parameters of the transmitter which must generate sufficient power to obtain high-quality images. For example, for a modern constellation of 27 ICEYE SAR spacecrafts (ICEYE, Finland), the peak radiated power is 3.2 kW.[1]

For this reason, non-radiating systems are considered to be a separate area of space radar development. In such systems, the role of a transmitter is performed by existing (third-party) satellites. The most elaborated of these is the option of using global navigation satellite systems (GNSS) as transmitters. In foreign literature this option has received its own name: GNSS reflectometry (GNSS-R) [2, 3]. This option was used, among other things, for altimetry of the sea surface [4]. Russian scientists have also proposed options for creating remote sensing equipment based on the use of GLONASS signals[2] in terms of building multi-position systems [5, 6], methods of signal processing in the aperture synthesis mode [7], the use of ground-based signal reception system for determining surface parameters [8], the use of aircraft for receiving and processing signals [9]. However, only one project has been realized in practical terms [10].

The results of ship detection on the background of water surface using GNSS signals as presented in [10–12] show that such detection is only possible when the aperture synthesis algorithm is implemented. [13, 14] also published data on successful detection of river vessels from GNSS signals using aperture synthesis.

In 2014, the TechDemoSat-1 satellite (SSTL, United Kingdom) was launched. It carries equipment to receive GNSS signals reflected from the sea surface and to determine wind speeds and the boundaries between the water surface and ice.

On September 28, 2015, the European Space Agency launched Spire nanosatellites (Spire Global, Scotland). It generates radar data for water, sea surface, ice cover, and also enable estimating ionosphere parameters using GNSS signals [15].

The NASA Cyclone Global Navigation Satellite System (CYGNSS) satellite constellation launched in December 2016 consists of 8 satellites and provides resolution in coherent accumulation mode up to 3.5 × 0.5 km with estimation of water and land surface parameters.[3]

GNSS-R satellites were also launched. They include: FSSCat [16], Chinese BuFeng-1 (BF-1) A/B satellites [17], Surrey Satellite Technology Ltd (SSTL) DoT-1 satellite [18], Fengyun-3E satellite [19]. The People's Republic of China launched the Jilin-1 Kuanfu 01C satellite on May 8, 2023, which receives GNSS signals reflected from the Earth's surface to determine average sea surface height, wave height, ice cover characteristics, surface wind parameters, and sea salinity.[4]

The Spire nanosatellite network is the most modern. It has more than 165 3U/6U microsatellites launched on the LEMUR platform. GNSS-R satellites on this platform collect 4 GB of data daily, which are received by more than thirty ground stations.[5]

Remote sensing based on reflected GNSS signals is being developed in such projects as PRETTY[6], HydroGNSS[7], SNOOPI[8], etc.

1. TASK STATEMENT

The task of 24/7 monitoring of the Earth's surface under any weather conditions needs to be resolved through the creation of a constellation of bistatic radars with a receiver on the spacecraft. In order to create such

[1] https://earth.esa.int/eogateway/missions/iceye. Accessed March 20, 2024.

[2] https://glonass-iac.ru/ (in Russ.). Accessed March 20, 2024.

[3] https://podaac.jpl.nasa.gov/CYGNSS. Accessed 20.03.2024.

[4] https://news.cgtn.com/news/2022-05-08/China-launches-first-bipolar-GNSS-R-ocean-survey-payload-19RYzG3bmCs/index.html. Accessed March 20, 2024.

[5] https://spirespaceservices.spire.com/. Accessed March 20, 2024.

[6] https://space.oscar.wmo.int/satellites/view/pretty. Accessed March 20, 2024.

[7] https://www.eoportal.org/satellite-missions/hydrognss. Accessed March 20, 2024.

[8] https://esto.nasa.gov/invest/snoopi. Accessed March 20, 2024.

promising Russian satellites, in order to resolve the task of building radar images of the Earth's surface, measure geoid height, detect broken ice fields, etc. based on the results of reception and processing of GNSS signals reflected from the surface, the method of optimal processing of reflected signals, signal energy, the structure of data reception and processing equipment, need to be defined, including the parameters of the antenna system.

We synthesized an algorithm for radar image formation in space bistatic SAR in the mode of receiving reflected GNSS satellite signals. This enabled us to obtain radar images of the disturbed surface near mirror reflection points. We will form an algorithm for an additive model of the observation equation including a useful signal $S(t)$ at the antenna input and noise $n(t)$, where t is time. In this case, we will assume that the mutual interference of signals is insignificant and can be accounted for in the receiver noise.

Let us distinguish an arbitrary bistatic pair ith receiver–kth transmitter (Fig. 1).

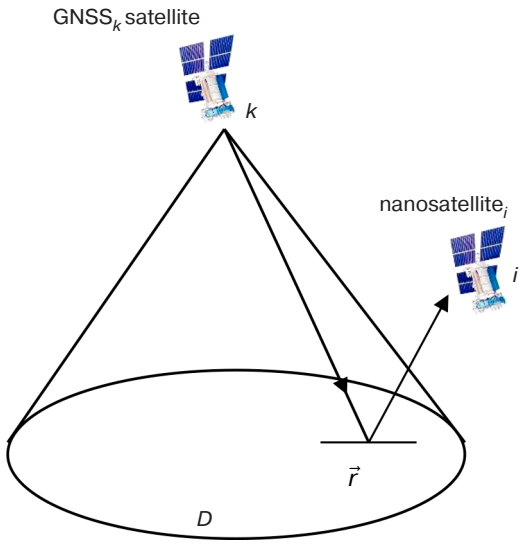

Fig. 1. Observation geometry. $\vec{r}$ is the reflecting point within the probed surface D

The signal of the kth GNSS satellite, reflected from the surface and received by the ith receiving antenna, after reflection from the surface point with coordinates are defined by the expression:

$$\begin{aligned}\dot{S}_{ik}(t,\vec{r}) &= \dot{K}_k(t,\vec{r})\dot{K}_i(t,\vec{r})\times \\ &\times \dot{G}_k(t,\vec{r})\dot{G}_i(t,\vec{r})\dot{F}_{ik}[t,\vec{r},\vec{\lambda}(\vec{r})]\times \\ &\times \dot{S}_{0k}[t-\tau_k(t,\vec{r})-\tau_i(t,\vec{r})]\times \\ &\times \exp\{j\omega_{0k}[t-\tau_k(t,\vec{r})-\tau_i(t,\vec{r})]\},\end{aligned} \quad (1)$$

where $\dot{S}_{ik}(t,\vec{r})$ is the trajectory signal; $\dot{K}_k(t,\vec{r})$ and $\dot{K}_i(t,\vec{r})$ are the coefficients which take into account signal attenuation and distortion during propagation through the atmosphere from the transmitting antenna to the surface point $\vec{r}$ and from the surface point $\vec{r}$ to the receiving antenna, respectively. $\dot{G}_k(t,\vec{r})$, $\dot{G}_i(t,\vec{r})$ are the complex functions which take into account the influence of the directivity diagram of the transmitting and receiving antennas. $\dot{F}_{ik}[t,\vec{r},\vec{\lambda}(\vec{r})]$ is the complex reflection coefficient of the element $\vec{r}$, depending on its electrophysical parameters $\vec{\lambda}(\vec{r})$ for the bistatic pair ik. $\dot{S}_{0k}(t)\exp(j\omega_{0k}t)$ is the signal emitted by the kth satellite, and $\omega_{0k}=2\pi f_{0k}$ is the carrier frequency of the emitted signal of the kth transmitter. Further, $\tau_k(t,\vec{r})$ and $\tau_i(t,\vec{r})$ is the delay time associated with the signal path from the transmitting antenna to the surface point with coordinates $\vec{r}$ and from the surface point to the receiving antenna, respectively.

For practical calculations of the reference functions in synthesizing the aperture in bistatic SAR, the change of the functions $\dot{G}(t,\vec{r})$ and $\dot{K}(t,\vec{r})$ for the time of pulse propagation can reasonably be neglected. The function $\dot{F}[t,\vec{\lambda}(t,\vec{r})]=\dot{F}[\vec{r},\vec{\lambda}(\vec{r})]$ will be considered constant over the observation interval. As a result, the signal $S_{Dik}(t)$ reflected from the probed surface D will be a real part of the limit value of the sum of signals reflected from its individual elements $\dot{S}_{ik}(t,\vec{r})$:

$$\begin{aligned}S_{Dik}(t) &= \\ &= \mathrm{Re}\int_D \dot{F}_{ik}[\vec{r},\vec{\lambda}(\vec{r})]\dot{K}_{ik}[t,\vec{r}]\dot{G}_{ik}[t,\vec{r}]\dot{S}_{0k}[t-\tau_{ik}(t,\vec{r})]\times \\ &\times \exp\{j\omega_{0k}[t-\tau_{ik}(t,\vec{r})]\}d\vec{r},\end{aligned} \quad (2)$$

where, for the convenience of perception, the products of the functions depending on the transmitter and receiver parameters are combined into one function with indices $(\cdot)_{ik}$.

Although reflection occurs from all surface elements for which the traces of the directivity diagrams of the transmitting and receiving antennas intersect, the greatest contribution will be made by components near the point of specular reflection [20].

A particular feature of the processing mode (2) is the determination of the difference of course between the direct and reflected signal. The processing of the direct GNSS signal and the signal reflected from the mirror area enables not only the surface parameters to be estimated, but also the current height of the geoid at this point to be calculated. The number of such mirror reflection points coincides with the number of visible GNSS satellites. The points themselves move in space with the mutual movement of the transmitter and receiver relative to the underlying surface.

Both foreign and Russian researchers [21–23] have demonstrated the possibility of resolving the task of

altitude measurement. The use of high-precision GNSS ephemerides allows us to resolve the task of altimetry with a high level of accuracy. For example, the motion parameters of the center of mass of the GLONASS GNSS satellites are determined with errors (at a probability level of 0.997) of no more than 0.5 m along the orbit, 0.2 m along the binormal to the orbit, and 0.1 m along the radius-vector.[9]

2. OPTIMAL SIGNAL PROCESSING IN BISTATIC SPACEBORNE RADAR SYSTEM

Without a loss of generality of the results, let us assume that the useful signal emitted by the navigation satellite, reflected from the Earth's surface and received on board the nanosatellite $\mathrm{Re}\,\dot{S}_{Dik}(t)$, is observed against the background of additive normal white noise $n_{ik}(t)$. The statistical characteristics thereof can be assumed to be the same for all pairs *i*th receiver–*k*th transmitter:

$$u_{ik}(t) = \mathrm{Re}\,\dot{S}_{Dik}(t) + n_{ik}(t). \tag{3}$$

Optimal estimates of surface $\vec{\lambda}(\vec{r})$ parameters contained in the reflected signal, for functionally-deterministic surface models can be found in the framework of the maximum likelihood method by means of the maximum of the functional:

$$p\left[u_{ik}(t) / \dot{F}_{ik}[\vec{r},\vec{\lambda}(\vec{r})]\right] = \\ = C\exp\left\{-\frac{1}{N_{0_{ik}}}\int_0^T [u_{ik}(t) - \mathrm{Re}\int_D \dot{F}_{ik}[\vec{r},\vec{\lambda}(\vec{r})]\dot{S}_{ik}(t,\vec{r})d\vec{r}]^2 dt\right\}, \tag{4}$$

where $N_{0_{ik}}$ is the additive noise power spectral density, T is the observation interval (aperture synthesis), C is the normalizing multiplier.

Let one of the parameters $\lambda(\vec{r})$ be estimated, if there is no a priori information about it or if it is distributed with maximum entropy (uniformly in the area Λ, $\lambda \in \Lambda$), then the optimal estimates are to be found from the solution of the variational equation $\frac{\delta\left\{p[u_{ik}(t) / \dot{F}_{ik}[\vec{r},\lambda(\vec{r})]]\right\}}{\delta\lambda(\vec{r})} = 0$. The variational equation occurs due to the fact that it is not a constant value of the parameter estimated, but a function of spatial coordinates $\dot{F}_{ik}[\vec{r},\lambda(\vec{r})]$.

After a number of calculations, the solution of Eq. (4), which defines the principle of aperture synthesis in bistatic radar system, can be written in compact form as follows:

$$\dot{Y}_{ik}(\vec{r}) = \int_0^T u_{ik}(t)\dot{S}^*_{ik}(t,\vec{r})dt = \\ = \int_D \dot{F}_{ik}[\vec{r},\vec{\lambda}(\vec{r})]\dot{\Psi}_{ik}(\vec{r},\vec{r}_1)d\vec{r}_1, \tag{5}$$

where $\dot{Y}_{ik}(\vec{r}) = \int_0^T u_{ik}(t)\dot{S}^*_{ik}(t,\vec{r})dt$ is the optimal output effect in a given bistatic pair, $\dot{\Psi}_{ik}(\vec{r},\vec{r}_1) = \int_0^T \dot{S}_{ik}(t,\vec{r})\dot{S}^*_{ik}(t,\vec{r}_1)dt$ is the spatial uncertainty function of bistatic SAR.

Processing result (5) is a radar image of the surface which contains information about its electrophysical parameters.

The formation of independent estimates for all bistatic pairs allows us to obtain $N = N_{\mathrm{KA}}N_{\mathrm{S}}$ measurements (4), wherein N_{KA} is the number of visible GNSS SC, N_{S} is the number of emitted (quasi)-orthogonal signals. For GNSS GLONASS[10] the signals L1OF, L1OC (L1OCd и L1OCp), L2q (L2OCd, L2OCp), L2OF, L3OC (L3OCd и L3OCp) at visibility of 10 navigation satellites enable us to obtain 80 values of $\dot{Y}_{ik}(\vec{r})$ (see the table).

As a result of processing (5), the output will be an additive mixture of four components:

- signal part for a specific signal of a given transmitter $\dot{S}_{ik}(t,\vec{r})$

$$\dot{Y}_{S_{ik}}(\vec{r}) = \int_D \dot{F}_{ik}[\vec{r},\vec{\lambda}(\vec{r})]\dot{\Psi}_{ik}(\vec{r},\vec{r}_1)d\vec{r}_1; \tag{6}$$

- noise component

$$\dot{Y}n_{ik}(\vec{r}) = \int_0^T n_{ik}(t)\dot{S}^*_{ik}(t,\vec{r})dt; \tag{7}$$

- interference component for the same satellite emitting M signals $\dot{S}^*_{imk}(t,\vec{r}_1)$ which do not coincide with $\dot{S}_{ik}(t,\vec{r})$:

$$\dot{Y}_{IS_{ik}}(\vec{r}) = \\ = \sum_{m=1\ldots M}\int_D \dot{F}_{ik}[\vec{r},\vec{\lambda}(\vec{r})]\int_0^T \dot{S}_{ik}(t,\vec{r})\dot{S}^*_{imk}(t,\vec{r}_1)dtd\vec{r}_1; \tag{8}$$

- inter-satellite interference component caused by the reception of signals from other GNSS satellites irradiating the D surface area:

[9] http://www.glonass-svoevp.ru/index.php?lang=ru (in Russ.). Accessed March 20, 2024.

[10] https://russianspacesystems.ru/bussines/navigation/glonass/interfeysnyy-kontrolnyy-dokument/ (in Russ.). Accessed March 20, 2024.

Table. Characteristics of GLONASS signals. *I* and *Q* are in-phase and quadrature components of the signal, respectively

Carrier frequency f_0, MHz	1602 + 0.5625k $k = -7 \ldots +6$		1600.995			1248.06			1246 + 0.4375k $k = -7 \ldots +6$		1202.025	
I/Q	Q	I	Q		I	Q		I	Q	I	Q	I
Type	L1OF (L1 CT)	L1SF (Ll BT)	L1OC [L1OCd]	L1OC [LOCp]	L1SC	L2q (L2OC) [L2KCИ (L2OCd)]	L2q (L2OC) [L2OCp]	L2SC	L2OF (L2 CT)	L2SF (L2 BT)	L3OC [L3OCp	L3OC [L3OCd]]
Strip, MHz	1.022	–	2.046	4.092	–	2.046	4.092	–	1.022	–	20.46	20.46
Average signal power $\bar{A}$, dBW	−161	–	−161.5	−161.5	–	−161.5	−161.5	–	−161	–	−101.5	−101.5

$$\dot{Y}_{in_{ik}}(\vec{r}) = \sum_{n=1\ldots N} \int_D \dot{F}_{ik}[\vec{r},\vec{\lambda}(\vec{r})] \int_0^T \dot{S}_{ik}(t,\vec{r})\dot{S}^*_{in}(t,\vec{r}_1)dtd\vec{r}_1. \quad (9)$$

The study of the influence of quasi-orthogonal signals, including the different trajectories of GNSS satellite motion, can be performed both numerically and experimentally. The experiment enables the statistical characteristics of noise and interference components to be estimated when comparing the effects at the correlator output obtained in an anechoic chamber for a single simulated GNSS satellite signal and the same effects when working on the signals of real GNSS satellites. Such an experiment, conducted at the All-Russian Research Institute of Physical-Technical and Radio-Technical Measurements[11] [24], showed that, in accordance with the law of large numbers, the combined effect (8)–(9) can be approximated by a normal random process. Consequently, these components can be accounted for using the simplified model (3) with a 1–2 dB increase in noise level.

3. ENERGY POTENTIAL OF BISTATIC SAR WITH THE RECEPTION OF REFLECTED GNSS SIGNALS

When calculating the energy parameters, we will assume that the receiver of the multi-position SAR performs optimal processing—matched filtering in accordance with (5). Then at the output of the processing system, two components will be formed: signal $\dot{Q}_s$ and noise $\dot{Q}_n$ components.

[11] https://www.vniiftri.ru/ (in Russ.). Accessed March 20, 2024.

Let us write down the power of the signal component P_s in the following form:

$$P_s = \frac{\lambda^2}{(4\pi)^3} \cdot \frac{P_{av} G_T}{R_1^2} \cdot \frac{G_R T_{Rs}}{R_2^2} \sigma^o \Delta s, \quad (10)$$

where P_{av} is the average power of the signal emitted by the transmitter. T_{Rs} is the time of receiver synthesis. R_1, R_2 is the distance from the reflecting point to the transmitter and receiver, respectively. G_T, G_R are the gain coefficients of the transmitting and receiving antenna, respectively, σ^o is the specific effective scattering area (SESA) of the surface, Δs is the resolution area size on the probed surface.

When surface specular reflection is used, the trace on the surface of the spatial uncertainty function of the navigation signal $\dot{\Psi}_{ik}(\vec{r},\vec{r}_1)$ should be used as the size of the area.

The noise component of the output effect (4) $\dot{Q}_n$ is determined by the interference power spectral density at the receiver input N_0:

$$N_0 = t_A k T_0, \quad (11)$$

where t_A is the relative noise temperature of the antenna, $k = 1.38 \cdot 10^{-23}$ J/K is the Boltzmann constant, T_0 is the antenna temperature.

In Eq. (10), the main parameters are determined by the observation geometry and the characteristics of the transmitters, i.e. the navigation satellites. Additionally, the specific effective surface scattering surface needs to be defined.

The mathematical model of reflection from the agitated sea surface is based on the two-scale surface model [25]. In order to describe the reflection of the navigation signal from the sea surface, the BA-PTSM

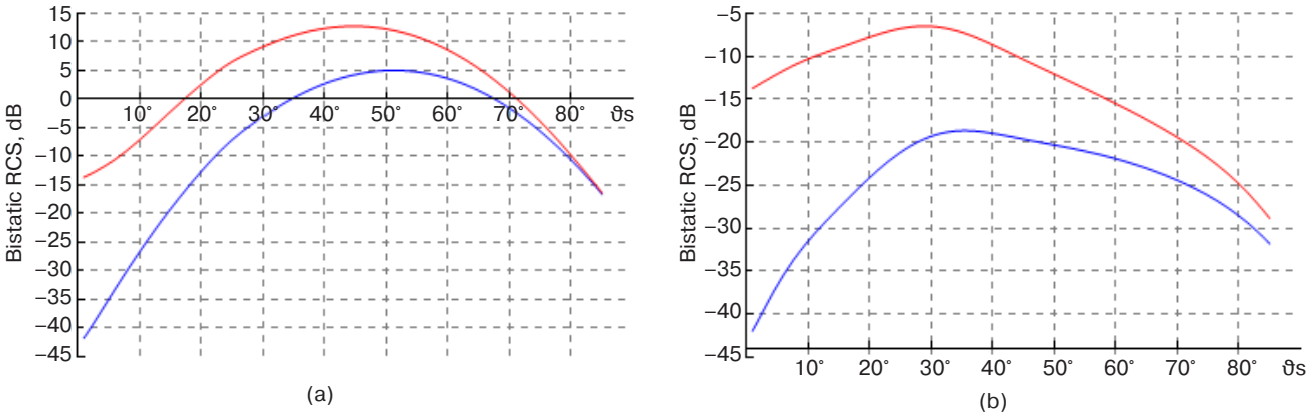

Fig. 2. Dependence of the SESA value at reception of the reflected signal with right circular polarization (red line) and left circular polarization (blue line) on the vertical scattering angle ϑs for the signal with frequency 1.58 GHz at the coinciding vertical projection of bistatic observation angle 45° and horizontal projection of bistatic angle 0° (a) and 30° (b) [26]

model [26] is proposed. This model takes into account the polarization of the signals and at the same time provides higher calculation speed while matching the results with the two-scale model. For this model, the results of calculating the SESA for the circular polarization of the GNSS satellite signal are shown in Fig. 2.

Experimentally obtained data can be used to estimate the energy parameters (Figs. 3 and 4).

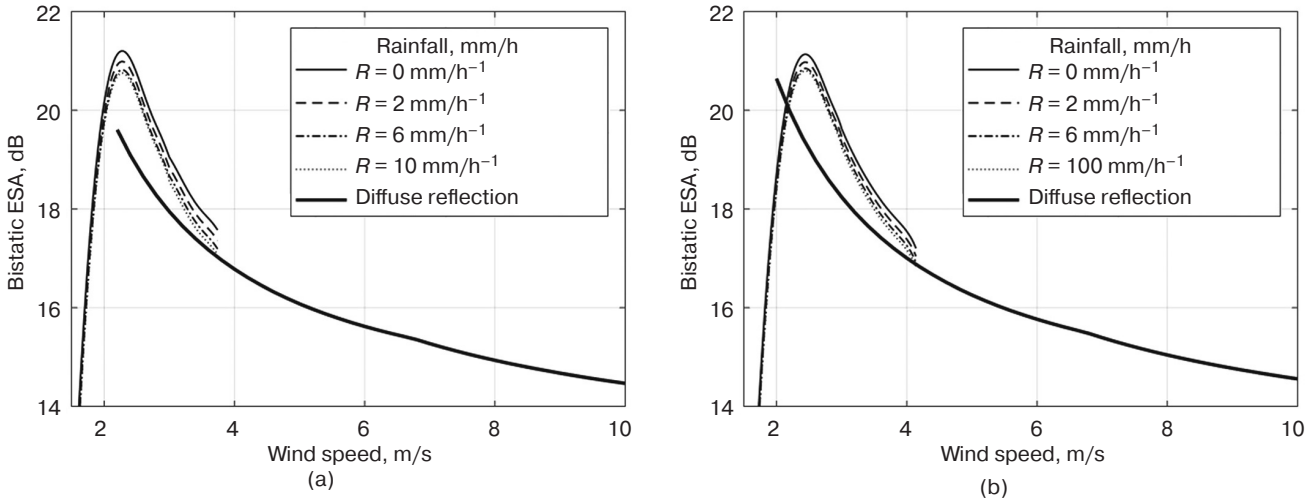

Fig. 3. Dependence of bistatic ESA of GPS[12] L1 signal for sea surface on the driving wind speed at different precipitation level *R* for the horizontal projection of bistatic angle 0° (a) and 30° (b), according to data [27]

The results of calculation (9) using data from [28] show that using an antenna with a gain of 14 dBi, it is possible to provide a signal-to-noise ratio of 4 dB for an accumulation time of 1 ms in regions up to 10° relative to the mirror reflection region. The results obtained are close to those obtained experimentally at wind speeds less than 5 m/s [29] (Fig. 5).

The optimum aperture synthesis time is limited by two factors. On the one hand, the signal accumulation needs to be achieved with a level sufficient to ensure the required accuracy of estimates of surface parameters and geoid height (at least 10 ms). On the other hand, the surface parameters should not change significantly during the synthesis time, in order that the complex reflection coefficient in Eq. (3) does not become a function of time. When placed on an ultra-small cubesat[13], the antenna gain will be no more than 10–16 dBi (size of the antenna corresponds to one face of the 3U-6U spacecraft), unless a design with an unfolding antenna is used, i.e. as on the SPIRE spacecraft. Taking into account the possibility of co-processing over visible satellites which may produce an additional 4–7 dB increase in signal-to-noise ratio, the aperture synthesis time can be reduced to 100 ms. This will greatly simplify the implementation of aperture synthesis on board.

[12] https://www.gps.gov/. Accessed March 20, 2024.
[13] https://www.nasa.gov/wp-content/uploads/2018/01/cubesatdesignspecificationrev14_12022-02-09.pdf. Accessed March 20, 2024.

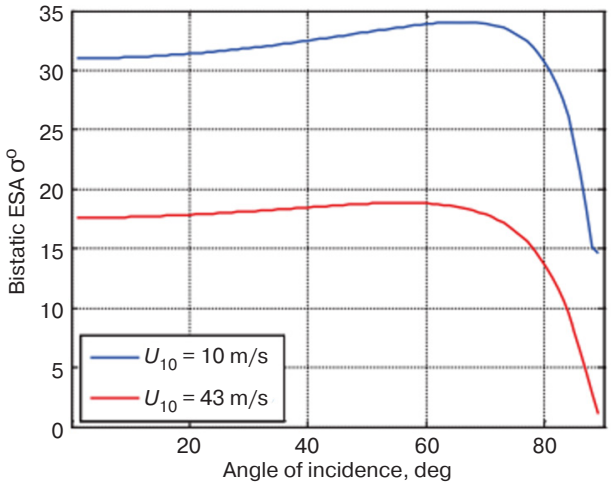

Fig. 4. Dependence of the bistatic ESA of the GPS L1 signal for the sea surface in the specular reflection region on the scattering angle for two driving wind speeds U_{10}, according to σ° [26][14]

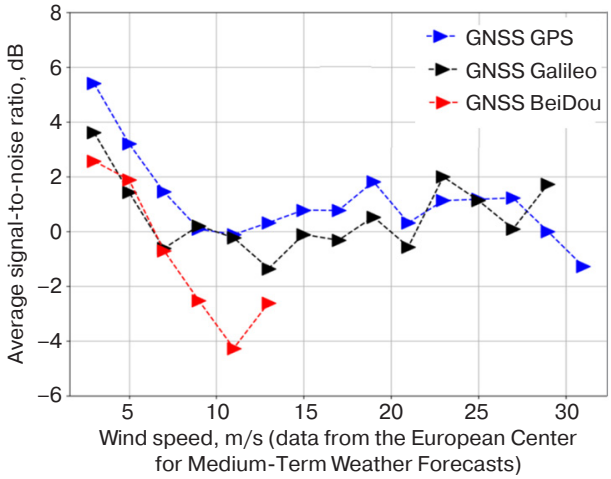

Fig. 5. Average values of signal-to-noise ratio at different wind speeds (for GNSS GPS, Galileo[15], BeiDou[16]) [29]

4. STRUCTURE OF ON-BOARD BISTATIC RADAR SYSTEM

For correct signal processing, the on-board radar must contain (Fig. 6):

- antenna system to receive the direct GNSS signal needed to form the reference signal (standard navigation antenna);
- antenna system for signal reception with left circular polarization, polarization separation not worse than 20 dB, gain not less than 10 dBi;
- software-defined receiver;
- standard spaceborne GNSS receiver with the ability to provide coordinate information for spacecraft position control. This information is used in the correlator to form reference functions, which will significantly reduce the requirements for onboard processing;
- data transmission channel with data storage device for data transmission to ground stations.

In order to increase signal-to-noise ratio, a patch antenna can reasonably be used. The size of the proposed antenna is larger than that used in CYGNSS (6 patch elements). The elements are arranged in a mosaic, but they can also be arranged in parallel, as in foreign GNSS-R, and thus reduce the size of the antenna on the satellite (Fig. 7).

[14] *Cyclone global navigation satellite system* (*CYGNSS*). Algorithm Theoretical Basis DocumentLevel 2 Wind Speed Retrieval. https://cygnss.engin.umich.edu/wp-content/uploads/sites/534/2021/07/148-0138-ATBD-L2-Wind-Speed-Retrieval-R6_release.pdf. Accessed March 20, 2024.

[15] https://galileognss.eu/. Accessed March 20, 2024.

[16] https://glonass-iac.ru/guide/gnss/beidou.php (in Russ.). Accessed March 20, 2024.

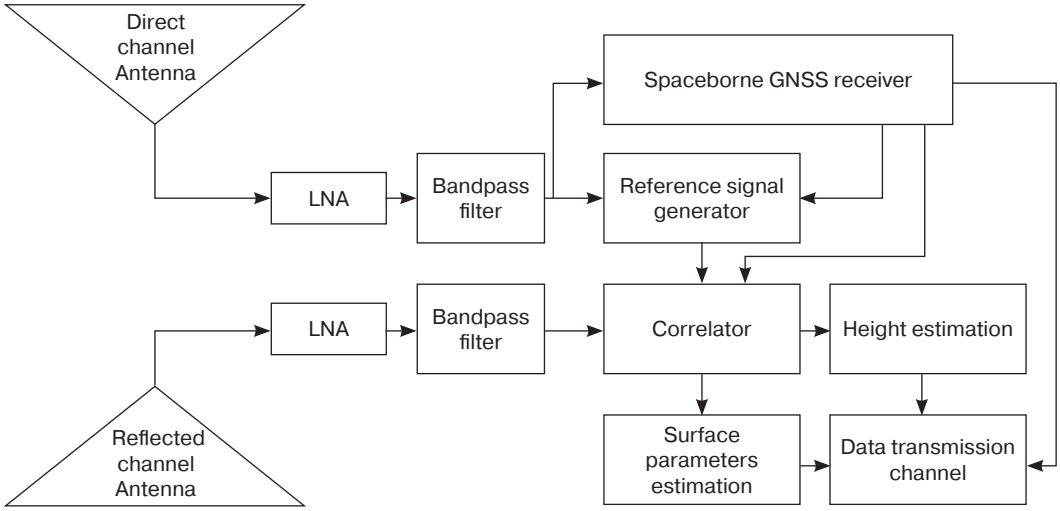

Fig. 6. Proposed structure of bistatic radar operating on GNSS signals reflected from the surface. LNA—low noise amplifier

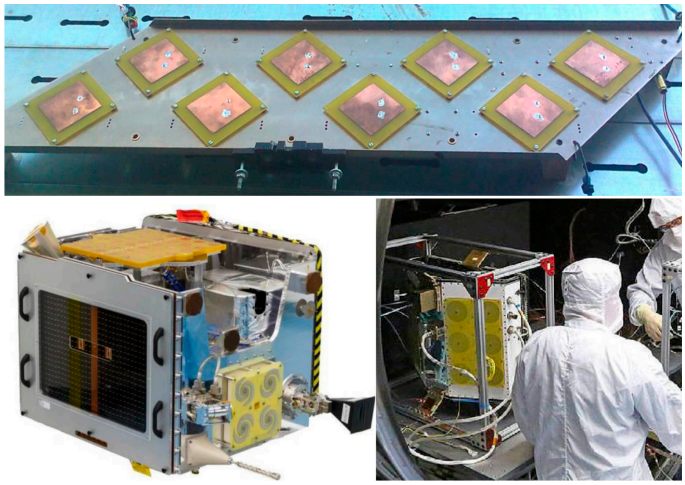

Fig. 7. Proposed patch antenna array model (top) [14], TDS-1 satellite antenna (bottom left) [11] and CYGNSS (bottom right)[17] [28]

It is advisable to have two antennas for receivers on spacecraft. They are directed to the left and right of the sub-satellite point at an angle of 30° relative to the vertical, in order to enable signals to be processed to the left and right of the track of the receiving spacecraft. In this case, the scheme in Fig. 6 adds one more receiving channel of the GNSS signal reflected from the surface.

5. WAYS TO INCREASE THE ENERGY POTENTIAL OF BISTATIC SAR

The main disadvantage of non-radiating radar is that the power of the transmitters is relatively low. In CYGNSS, the simplest method of providing the required power is to process the signal in the mirror reflection region. This provides a 15–30 dB increase in signal strength relative to other regions. The size of the region which makes the main contribution to the reflected signal depends not only on the observation geometry, but also on the characteristics of the underlying surface (Fig. 8) [30]. Sea ice, lake surface and swampy terrain are characterized by a small reflection area in the delay–Doppler shift coordinates due to specular reflection. Vegetation cover and open sea are characterized by a wide reflection area. Consequently, information about the type of reflecting surface is contained not only in the absolute value of the reflected signal power, but also in its distribution in the delay–Doppler shift coordinates. This makes it possible for new methods to be created for analyzing radar images to determine the water-ice situation.

[17] https://www.eoportal.org/satellite-missions/techdemosat-1#spacecraft. Accessed March 20, 2024.

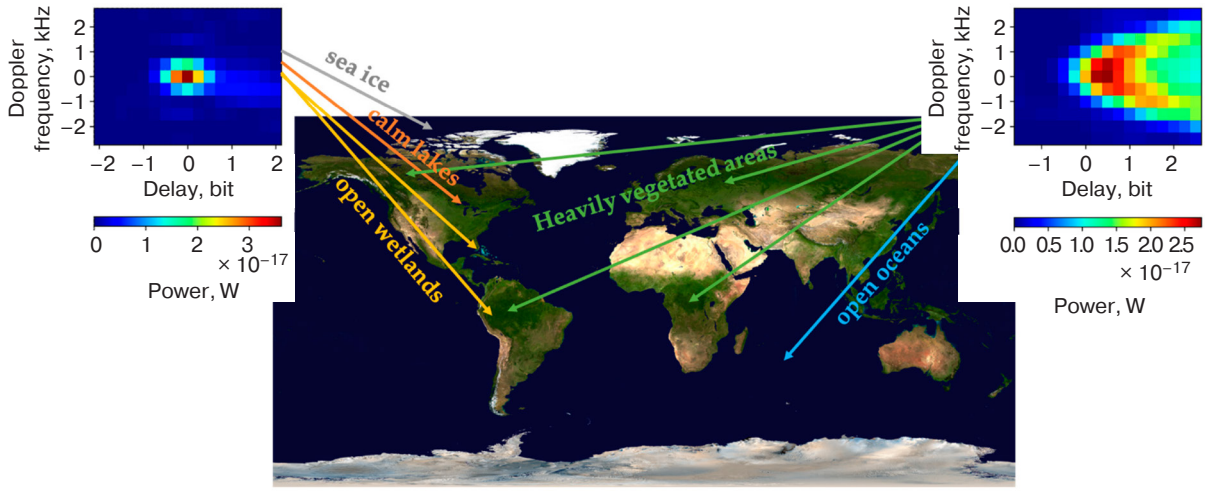

Fig. 8. Two example images in delay–Doppler shift coordinates for two different types of surfaces [30]

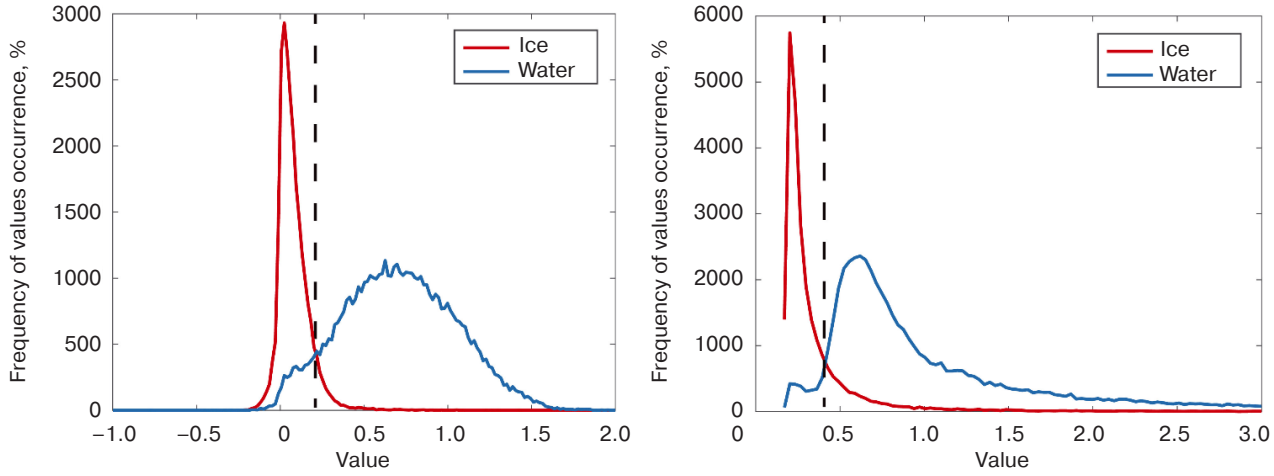

Fig. 9. Histograms of reflection power distribution in the range–Doppler shift coordinates (left) and the leading edge of the reflected pulse (right)

Another indication of distinguishing the GNSS signal reflected from water and ice can be a histogram of the level of the reflected signal from the type of surface (Fig. 9) [31].

The synthesis of the optimal co-processing algorithm is performed by taking into account the electrodynamic models of the surface when it is observed at different angles and at different carrier frequencies [32].

In order to increase the signal-to-noise ratio, required in order to improve the quality of estimates, we propose the use of coherent signal accumulation (in the mode of synthesizing the antenna aperture). This will make it possible to observe and equalize the spatial resolution in the range and azimuthal directions in a wide range of angles.

Additional opportunities are provided by receiving the signals of all visible GNSS satellites, their separate processing (aperture synthesis) and subsequent aggregation of measurements at the stage of secondary processing (estimation of surface parameters, object detection and radar imaging).

In contrast to the methods of processing the reflected GNSS signals described in the literature, signals at all carrier frequencies need to be processed. This makes it possible to generate independent data on the surface reflectivity and correct ionospheric distortions. This is particularly important when determining the geoid height for a sub-satellite point or a specular reflection point.

CONCLUSIONS

The study analyzed systems of remote sensing of the Earth surface by reflected signals of navigation satellites. It also showed that foreign constellations of such satellites operate in orbit, thus resolving the tasks of determining the parameters of the water surface and soil. Data from these satellites is publicly available and can be analyzed. Taking into account the limited capabilities for creating meteorological satellite constellations, satellites for water surface monitoring and geoid height determination, based

on reception of reflected signals of satellite navigation systems, enable a number of important scientific and practical tasks to be resolved. This paper presents an algorithm for the optimal processing of reflected signals of navigation systems, and takes into account the particular features of GNSS satellite operation, including the presence of interference component. The numerically calculated values of the energy potential of bistatic SAR for circular polarization signals coincide with the experimental values given in foreign literature.

The study proposes a choice of aperture synthesis time of the order of 100 ms. This takes into account the constancy of the reflecting surface parameters. A further increase of signal-to-noise ratio can be achieved by means of joint processing over the whole visible constellation.

The paper also proposes a structure of onboard bistatic radar, which, unlike known analogs, uses a navigation receiver to form a reference signal. The use of delays and Doppler frequency shifts calculated in the navigation equipment allows us to simplify the signal correlator. This also enables the load on the software-defined receiver to be reduced while maintaining the required quality of estimates.

ACKNOWLEDGMENTS

The study was financially supported by the Russian Science Foundation, grant No. 23-67-10007.

Authors' contributions

A.V. Ksendzuk—developing aims and objectives, theoretical background, processing methods, and energy potential.

V.F. Fateev—the research idea, developing the structure of on-board bistatic radar system, and formulating the conclusions.

REFERENCES

1. Krieger G., Moreira A., Fiedler H., et al. TanDEM-X: A satellite formation for high-resolution SAR interferometry. *IEEE Trans. Geosci. Remote Sens*. 2007;45(11):3317–3341. https://doi.org/10.1109/TGRS.2007.900693
2. Hall C.D., Cordey R.A. Multistatic scatterometry. In: *International Geoscience and Remote Sensing Symposium, 'Remote Sensing: Moving Toward the 21st Century'*. IEEE. 1988. V. 1. P. 561–562. https://doi.org/10.1109/IGARSS.1988.570200
3. Cardellach E., Fabra F., Nogués-Correig O., et al. GNSS-R ground-based and airborne campaigns for ocean, land, ice, and snow techniques: Application to the GOLD-RTR data sets. *Radio Sci*. 2011;46(6):RS0C04. http://doi.org/10.1029/2011RS004683
4. Martin-Neira M. A passive reflectometry and interferometry system (PARIS): Application to ocean altimetry. *ESA J*. 1993;17(4):331–355.
5. Ksendzuk A.V. Use of GLONASS/GPS satellite navigation systems for remote surface sensing. *Elektromagnitnye volny i elektronnye sistemy = Electromagnetic Waves and Electronic Systems*. 2003;8(5):8–15 (in Russ.).
6. Fateev V.F., Sakhno I.V. Application of navigating space vehicles GPS/GLONASS in structure multi-position radar the review of a terrestrial surface. *Izvestiya vysshikh uchebnykh zavedenii. Priborostroenie = J. Instrument Eng.* 2004;47(3):27–30 (in Russ.).
7. Fateev V.F., Sakhno I.V. *Method for Producing Radiolocation Image of Earth Surface by Means of Using Multi-Positional Radiolocation System with Synthesized Aperture of Antenna*: RF Pat. 2278398. Publ. 20.06.2006 (in Russ.).
8. Fateev V.F., Ksendzuk A.V. *Ground-Space Radar System*: RF Pat. 113022. Publ. 27.01.2012 (in Russ.).
9. Baholdin V.S., Gavril D.A., Shaldaev A.V. Algorithms of pattern SAR images of the Earth surface with the use of GLONASS signals. *Izvestiya vysshikh uchebnykh zavedenii. Priborostroenie = J. Instrument Eng.* 2012;55(9):24–29 (in Russ.).
10. Ksendzuk A.V., Fateev V.F., Gerasimov P.A., Novikov V.A. Multiposition radar coprocessing techniques. Experimental results. In: *Radar Research of Natural Environments*: *Proceedings of the 28th All-Russian Symposium*. St. Petersburg: Mozhaisky Military Space Academy. 2013;10(2):218–222 (in Russ.).
11. Di Simone A., Park H., Riccio D., Camps A. Sea target detection using spaceborne GNSS-R delay-Doppler maps: Theory and experimental proof of concept using TDS-1 data. *IEEE Journal of Selected Topics in Applied Earth Observations and Remote Sensing*. 2017;10(9):4237–4255. https://doi.org/10.1109/JSTARS.2017.2705350
12. Hu C., Benson C.R., Park H., et al. Detecting targets above the Earth's surface using GNSS-R delay Doppler maps: Results from TDS-1. *Remote Sens*. 2019;11(19):2327. https://doi.org/10.3390/rs11192327
13. Fateev V.F., Ksendzuk A.V., Obukhov P.S., et al. Multi-position non-radiating SAR with GNSS GLONASS transmitters. *Elektromagnitnye volny i elektronnye sistemy = Electromagnetic Waves and Electronic Systems*. 2012;17(5):62–68 (in Russ.).
14. Fateev V.F., Ksendzuk A.V., Obukhov P.S., et al. Experimental bistatic radar complex. *Elektromagnitnye volny i elektronnye sistemy = Electromagnetic Waves and Electronic Systems*. 2012;17(5):58–61 (in Russ.).
15. Freeman V., Masters D., Jales P., et al. Earth Surface Monitoring with Spire's New GNSS Reflectometry (GNSS-R) CubeSats. In: *22nd EGU General Assembly Conference Abstracts*. 2020. id. 13766. https://doi.org/10.5194/egusphere-egu2020-13766
16. Camps A., Golkar A., Gutierrez A., et al. Fsscat, the 2017 Copernicus Masters' "Esa Sentinel Small Satellite Challenge" Winner: A federated polar and soil moisture tandem mission based on 6U Cubesats. In: *IGARSS 2018 IEEE International Geoscience and Remote Sensing Symposium.* IEEE; 2018. P. 8285–8287. https://doi.org/10.1109/IGARSS.2018.8518405
17. Jing C., Niu X., Duan C., et al. Sea surface wind speed retrieval from the first Chinese GNSS-R mission: Technique and preliminary results. *Remote Sens*. 2019;11(24):3013. https://doi.org/10.3390/rs11243013

18. Unwin M., Rawinson J., King L., et al. GNSS-reflectometry activities on the DoT-1 microsatellite in preparation for the hydrognss mission. In: *2021 IEEE International Geoscience and Remote Sensing Symposium IGARSS*. IEEE; 2021. P. 1288–1290. https://doi.org/10.1109/IGARSS47720.2021.9554352
19. Xia J., Bai W., Sun Y., et al. Calibration and wind speed retrieval for the Fengyun-3 E Meteorological Satellite GNSS-R Mission. In: *2021 IEEE Specialist Meeting on Reflectometry using GNSS and other Signals of Opportunity* (*GNSS+R*). IEEE; 2021. P. 25–28. https://doi.org/10.1109/GNSSR53802.2021.9617699
20. Cheng Z., Jin T., Chang X., et al. Evaluation of spaceborne GNSS-R based sea surface altimetry using multiple constellation signals. *Front. Earth Sci*. 2023;10:1079255. https://doi.org/10.3389/feart.2022.1079255
21. Munoz-Martin J.F., Portero A.P., Camps A., et al. Snow and ice thickness retrievals using GNSS-R: Preliminary results of the MOSAiC experiment. *Remote Sens*. 2020;12(24):4038. https://doi.org/10.3390/rs12244038
22. Nogués O.C., Munoz-Martin J.F., Park H., et al. Improved GNSS-R altimetry methods: Theory and experimental demonstration using airborne dual frequency data from the microwave interferometric reflectometer (MIR). *Remote Sens*. 2021;13(20):4186. https://doi.org/10.3390/rs13204186
23. Fateev V.F., Lopatin V.P. Space bistatic radar to monitor the ocean surface profile based on GNSS signals. *Izvestiya vysshikh uchebnykh zavedenii. Priborostroenie = J. Instrument Eng.* 2019;62(5):484–491 (in Russ.). https://doi.org/10.17586/0021-3454-2019-62-5-484-491
24. Lopatin V.P., Fateev V.F. Study of a bistatic radiolocation system on the basis of GPS/GLONASS signals in echo-free camera. *Proceedings of the Mozhaisky Military Aerospace Academy*. 2019;670:64–68 (in Russ.).
25. Volosyuk V.K., Kravchenko V.F. *Statisticheskaya teoriya radiotekhnicheskikh sistem distantsionnogo zondirovaniya i radiolokatsii* (*Statistical Theory of Radio-engineering Systems of Remote Sensing and Radiolocation*). Moscow: Fizmatlit; 2008. 351 p. (in Russ.).
26. Di Martino G., Di Simone A., Iodice A., Riccio D. Bistatic scattering from anisotropic rough surfaces via a closed-form two-scale model. *IEEE Trans. Geosci. Remote Sens*. 2020;59(5):3656–3671. https://doi.org/10.1109/TGRS.2020.3021784
27. Asgarimehr M., Zavorotny V.U., Wickert J., Reich S. Can GNSS reflectometry detect precipitation over oceans? *Geophys. Res. Lett.* 2018;45(22):12,585–12,592. https://doi.org/10.1029/2018GL079708
28. Gleason S., Ruf C.S., O'Brien A.J., McKague D.S. The CYGNSS Level 1 calibration algorithm and error analysis based on on-orbit measurements. *IEEE Journal of Selected Topics in Applied Earth Observations and Remote Sensing*. 2019;12(1):37–49. https://doi.org/10.1109/JSTARS.2018.2832981
29. Nan Y., Ye S., Liu J., et al. Signal-to-noise ratio analyses of spaceborne GNSS-reflectometry from Galileo and BeiDou satellites. *Remote Sens*. 2022;14(1):35. https://doi.org/10.3390/rs14010035
30. Rodriguez-Alvarez N., Munoz-Martin J.F., Morris M. Latest Advances in the Global Navigation Satellite System—Reflectometry (GNSS-R) Field. *Remote Sens*. 2023;15(8):2157. https://doi.org/10.3390/rs15082157
31. Cartwright J., Banks Ch.J., Srokosz M. Sea Ice Detection Using GNSS-R Data From TechDemoSat-1. *JGR Oceans*. 2019. V. 124. Iss. 8. P. 5801–5810. https://doi.org/10.1029/2019JC015327
32. Potapov A.A., Kuznetsov V.A., Alikulov E.A. Methods for Complexing Images Formed by Multi-Band Synthetic Aperture Radars. *Izvestiya vysshikh uchebnykh zavedenii Rossii. Radioelektronika = Journal of the Russian Universities. Radioelectronics*. 2021;24(3):6–21 (in Russ.). https://doi.org/10.32603/1993-8985-2021-24-3-6-21

СПИСОК ЛИТЕРАТУРЫ

1. Krieger G., Moreira A., Fiedler H., et al. TanDEM-X: A satellite formation for high-resolution SAR interferometry. *IEEE Trans. Geosci. Remote Sens*. 2007;45(11):3317–3341. https://doi.org/10.1109/TGRS.2007.900693
2. Hall C.D., Cordey R.A. Multistatic scatterometry. In: *International Geoscience and Remote Sensing Symposium, 'Remote Sensing: Moving Toward the 21st Century'*. IEEE. 1988. V. 1. P. 561–562. https://doi.org/10.1109/IGARSS.1988.570200
3. Cardellach E., Fabra F., Nogués-Correig O., et al. GNSS-R ground-based and airborne campaigns for ocean, land, ice, and snow techniques: Application to the GOLD-RTR data sets. *Radio Sci*. 2011;46(6):RS0C04. http://doi.org/10.1029/2011RS004683
4. Martin-Neira M. A passive reflectometry and interferometry system (PARIS): Application to ocean altimetry. *ESA J*. 1993;17(4):331–355.
5. Ксендзук А.В. Использование спутниковых навигационных систем ГЛОНАСС/GPS для дистанционного зондирования поверхности. *Электромагнитные волны и электронные системы.* 2003;8(5):8–15.
6. Фатеев В.Ф., Сахно И.В. Применение навигационных КА GPS/ГЛОНАСС в составе многопозиционных РЛС обзора земной поверхности. *Известия высших учебных заведений. Приборостроение.* 2004;47(3):27–30.
7. Фатеев В.Ф., Сахно И.В. *Способ получения радиолокационного изображения земной поверхности при помощи многопозиционной радиолокационной системы с синтезированной апертурой антенны*: пат. № 2278398 РФ. Заявка № 2004121076/092006; заявл. 06.07.2004; опубл. 20.06.2006.
8. Фатеев В.Ф., Ксендзук А.В. *Наземно-космическая радиолокационная система*: пат. № 113022 РФ. Заявка № 2010154058/07; заявл. 29.12.20104; опубл. 27.01.2012.
9. Бахолдин В.С., Гаврил Д.А., Шалдаев А.В. Алгоритмы формирования радиолокационных изображений земной поверхности при использовании сигналов ГЛОНАСС. *Известия высших учебных заведений. Приборостроение*. 2012;55(9):24–29.

10. Ксендзук А.В., Фатеев В.Ф., Герасимов П.А., Новиков В.А. Совместная обработка в многопозиционных РСА. Результаты экспериментальных исследований. В сб.: *Радиолокационное исследование природных сред: труды XXVIII Всероссийского симпозиума*. СПб.: ВКА имени А.Ф. Можайского. 2013;10(2):218–222.
11. Di Simone A., Park H., Riccio D., Camps A. Sea target detection using spaceborne GNSS-R delay-Doppler maps: Theory and experimental proof of concept using TDS-1 data. *IEEE Journal of Selected Topics in Applied Earth Observations and Remote Sensing*. 2017;10(9):4237–4255. https://doi.org/10.1109/JSTARS.2017.2705350
12. Hu C., Benson C.R., Park H., et al. Detecting targets above the Earth's surface using GNSS-R delay Doppler maps: Results from TDS-1. *Remote Sens*. 2019;11(19):2327. https://doi.org/10.3390/rs11192327
13. Фатеев В.Ф., Ксендзук А.В., Обухов П.С., Крапивкин Г.И., Тимошенко Г.В., Король Г.Н., Фатеев О.В., Новиков В.А., Герасимов П.А., Шахалов К.С. Многопозиционная радиолокационная система с синтезированием апертуры антенны по отраженным сигналам ГНСС «ГЛОНАСС». *Электромагнитные волны и электронные системы*. 2012;17(5):62–68.
14. Фатеев В.Ф., Ксендзук А.В., Обухов П.С., Крапивкин Г.И., Тимошенко Г.В., Король Г.Н., Новиков В.А., Герасимов П.А., Шахалов К.С. Экспериментальный бистатический радиолокационный комплекс. *Электромагнитные волны и электронные системы*. 2012;17(5):58–61.
15. Freeman V., Masters D., Jales P., et al. Earth Surface Monitoring with Spire's New GNSS Reflectometry (GNSS-R) CubeSats. In: *22nd EGU General Assembly Conference Abstracts*. 2020. id. 13766. https://doi.org/10.5194/egusphere-egu2020-13766
16. Camps A., Golkar A., Gutierrez A., et al. Fsscat, the 2017 Copernicus Masters' "Esa Sentinel Small Satellite Challenge" Winner: A federated polar and soil moisture tandem mission based on 6U Cubesats. In: *IGARSS 2018 IEEE International Geoscience and Remote Sensing Symposium.* IEEE; 2018. P. 8285–8287. https://doi.org/10.1109/IGARSS.2018.8518405
17. Jing C., Niu X., Duan C., et al. Sea surface wind speed retrieval from the first Chinese GNSS-R mission: Technique and preliminary results. *Remote Sens*. 2019;11(24):3013. https://doi.org/10.3390/rs11243013
18. Unwin M., Rawinson J., King L., et al. GNSS-reflectometry activities on the DoT-1 microsatellite in preparation for the hydrognss mission. In: *2021 IEEE International Geoscience and Remote Sensing Symposium IGARSS*. IEEE; 2021. P. 1288–1290. https://doi.org/10.1109/IGARSS47720.2021.9554352
19. Xia J., Bai W., Sun Y., et al. Calibration and wind speed retrieval for the Fengyun-3 E Meteorological Satellite GNSS-R Mission. In: *2021 IEEE Specialist Meeting on Reflectometry using GNSS and other Signals of Opportunity* (*GNSS+R*). IEEE; 2021. P. 25–28. https://doi.org/10.1109/GNSSR53802.2021.9617699
20. Cheng Z., Jin T., Chang X., et al. Evaluation of spaceborne GNSS-R based sea surface altimetry using multiple constellation signals. *Front. Earth Sci*. 2023;10:1079255. https://doi.org/10.3389/feart.2022.1079255
21. Munoz-Martin J.F., Portero A.P., Camps A., et al. Snow and ice thickness retrievals using GNSS-R: Preliminary results of the MOSAiC experiment. *Remote Sens*. 2020;12(24):4038. https://doi.org/10.3390/rs12244038
22. Nogués O.C., Munoz-Martin J.F., Park H., et al. Improved GNSS-R altimetry methods: Theory and experimental demonstration using airborne dual frequency data from the microwave interferometric reflectometer (MIR). *Remote Sens*. 2021;13(20):4186. https://doi.org/10.3390/rs13204186
23. Фатеев В.Ф., Лопатин В.П. Космический бистатический радиолокатор контроля профиля поверхности океана на основе сигналов ГНСС. *Известия высших учебных заведений. Приборостроение.* 2019;62(5):484–491. https://doi.org/10.17586/0021-3454-2019-62-5-484-491
24. Лопатин В.П., Фатеев В.Ф. Исследование бистатической радиолокационной системы на основе сигналов GPS/ГЛОНАСС в безэховой камере. *Труды Военно-космической академии имени А.Ф. Можайского*. 2019;670:64–68.
25. Волосюк В.К., Кравченко В.Ф. *Статистическая теория радиотехнических систем дистанционного зондирования и радиолокации.* М.: Физматлит; 2008. 351 с.
26. Di Martino G., Di Simone A., Iodice A., Riccio D. Bistatic scattering from anisotropic rough surfaces via a closed-form two-scale model. *IEEE Trans. Geosci. Remote Sens*. 2020;59(5):3656–3671. https://doi.org/10.1109/TGRS.2020.3021784
27. Asgarimehr M., Zavorotny V.U., Wickert J., Reich S. Can GNSS reflectometry detect precipitation over oceans? *Geophys. Res. Lett.* 2018;45(22):12585–12592. https://doi.org/10.1029/2018GL079708
28. Gleason S., Ruf C.S., O'Brien A.J., McKague D.S. The CYGNSS Level 1 calibration algorithm and error analysis based on on-orbit measurements. *IEEE Journal of Selected Topics in Applied Earth Observations and Remote Sensing*. 2019;12(1):37–49. https://doi.org/10.1109/JSTARS.2018.2832981
29. Nan Y., Ye S., Liu J., et al. Signal-to-noise ratio analyses of spaceborne GNSS-reflectometry from Galileo and BeiDou satellites. *Remote Sens*. 2022;14(1):35. https://doi.org/10.3390/rs14010035
30. Rodriguez-Alvarez N., Munoz-Martin J.F., Morris M. Latest Advances in the Global Navigation Satellite System—Reflectometry (GNSS-R) Field. *Remote Sens*. 2023;15(8):2157. https://doi.org/10.3390/rs15082157
31. Cartwright J., Banks Ch.J., Srokosz M. Sea Ice Detection Using GNSS-R Data From TechDemoSat-1. *JGR Oceans*. 2019. V. 124. Iss. 8. P. 5801–5810. https://doi.org/10.1029/2019JC015327
32. Потапов А.А., Кузнецов В.А., Аликулов Е.А. Анализ способов комплексирования изображений, формируемых многодиапазонными радиолокационными станциями с синтезированной апертурой. *Известия высших учебных заведений России. Радиоэлектроника*. 2021;24(3):6–21. https://doi.org/10.32603/1993-8985-2021-24-3-6-21

About the authors

Alexander V. Ksendzuk, Dr. Sci. (Eng.), Head of Department Radioelectronic systems, Institute of Radio Electronics and Informatics, MIREA – Russian Technological University (78, Vernadskogo pr., Moscow, 119454 Russia). E-mail: ks_alex@mail.ru. Scopus Author ID 56628472300, RSCI SPIN-code 2389-6036, https://orcid.org/0009-0001-7084-1433, https://www.researchgate.net/profile/Alexander-Ksendzuk-2

Vyacheslav F. Fateev, Dr. Sci. (Eng.), Professor, Honored Scientist of the Russian Federation, Head of Scientific and Technical Center for Metrological Support of Ground and Space Gravimetry, Russian Metrological Institute of Technical Physics and Radioengineering (VNIIFTRI) (industrial zone of VNIIFTRI, settlement Mendeleevo, Solnechnogorsk, Moscow oblast, 141570 Russia). E-mail: office@vniiftri.ru. Scopus Author ID 56442213300, RSCI SPIN-code 5385-8126, https://orcid.org/0000-0001-7902-0212

Об авторах

Ксендзук Александр Владимирович, д.т.н., заведующий базовой кафедрой № 346 – радиоэлектронных систем, Институт радиоэлектроники и информатики, ФГБОУ ВО «МИРЭА – Российский технологический университет» (119454, Россия, Москва, пр-т Вернадского, д. 78). E-mail: ks_alex@mail.ru. Scopus Author ID 56628472300, SPIN-код РИНЦ 2389-6036, https://orcid.org/0009-0001-7084-1433, https://www.researchgate.net/profile/Alexander-Ksendzuk-2

Фатеев Вячеслав Филиппович, д.т.н., профессор, Заслуженный деятель науки РФ, начальник научно-технического центра «Метрологического обеспечения наземной и космической гравиметрии», ФГУП «Всероссийский научно-исследовательский институт физико-технических и радиотехнических измерений» (ФГУП «ВНИИФТРИ») (141570, Россия, Московская область, г. Солнечногорск, рабочий поселок Менделеево (промзона ВНИИФТРИ). E-mail: office@vniiftri.ru. Scopus Author ID 56442213300, SPIN-код РИНЦ 5385-8126, https://orcid.org/0000-0001-7902-0212

Translated from Russian into English by Lyudmila O. Bychkova
Edited for English language and spelling by Dr. David Mossop